ISSN 0030-400X, Optics and Spectroscopy, 2023, Vol. 131, No. 8, pp. 735–742. © Pleiades Publishing, Ltd., 2023.
Russian Text © The Author(s), 2022, published in Optika i Spektroskopiya, 2022, Vol. 130, No. 5, pp. 779–786.
English Text © Ioffe Institute, 2023.

Direct Laser Writing and Investigation of Optofluidic Elements inside Nanoporous Silicate Matrix

A. S. Shishkina[a], Y. I. Yandybaeva[a], V. A. Yakimuk[a], Yazan Alsaif[a], R. A. Zakoldaev[a,*], and O. V. Andreeva[a]

[a] *ITMO University, St. Petersburg, 197101 Russia*

**e-mail: zakoldaev@gmail.com*

Received November 3, 2021; revised December 8, 2021; accepted February 7, 2022

Abstract—The paper demonstrates direct laser writing by femtosecond laser pulses ($\lambda = 1030$ nm, $\tau = 220$ fs, $\nu = 200$ kHz) of functional optofluidic elements inside a nanoporous silicate matrix (NPSM). The influence of focused laser pulses led to the compaction of the nanoporous frame, which made it possible to fabricate barriers for the isolation of nanoporous cells and channel optical waveguides. The writing of microchannels in the mode of decompression of a nanoporous matrix with subsequent purification of debris area in distilled water under the action of ultrasound is also demonstrated. For each type of elements, the dependences of geometric characteristics on the energy parameters of laser radiation are established. The methods of testing the elements were also developed—checking the permeability of the barrier, the entering of laser radiation into channel waveguides.

Keywords: Direct laser writing, femtosecond laser pulses, barriers, waveguide, microchannel, porous silicate matrix, nanopores

DOI: 10.1134/S0030400X23060152

INTRODUCTION

Direct laser writing by using ultrashort laser pulses has been proven as a flexible and efficient tool for integration of solid elements of photonics [1, 2], micro- [3, 4] and nanofluidics [5] in various optic materials. Typical representatives of such elements are optical waveguides [6], nanogratings [7] and microchannels [8]. The trend of modern studies is directed to integration of functional optofluidic elements on a single glass matrix. Such integrated systems are demanded for creation of the Lab-on-a-chip [9], electrofluidic systems [10], micromechanical systems [11] and intelligent smartphones [12]. Miniaturization of the devices leads to reduction of the volumes of necessary reagents/analytes and increases sensibility [13].

Usually, direct laser writing is performed in solid optical media: fused silica [8], diamonds [14] or polymers [15]. The studies performed by a team of T.T. Fernandez etal. [16], have shown that selection of the glass composition for writing channel waveguides has a strong effect for the waveguide properties—optical losses, aspect ratio and refraction index contrast. We consider an alternative base for the integration of optofluidic elements—a nanoporous silicate matrix (NPSM) [17]. These matrices are optically transparent and highly resistant against physical and chemical effects, and the nanoporous structure allows to set the properties of formed elements within a wide range.

The article demonstrates the possibility of direct laser writing by using femtosecond laser pulses for three types of functional elements—isolated nanoporous cells, channel optical waveguides and microchannels in NPSM. Main geometrical characteristics of the elements are determined based on the parameters of laser radiation. The test procedures are proposed for the recorded elements.

EXPERIMENTAL PART

Plane-parallel plates of NPSM of the size 15 × 20 × 1 mm (Fig. 1a), with average pore size 17 nm, porosity ~50% and composition (by weight) $91.4SiO_2$–$7.4B_2O_3$–$1.2Na_2O$ were used as a material for laser writing [18]. NPSM plates have a high transmission within the range of 600–1100 nm (Fig. 1b).

Laser writing in NPSM plates was performed on the experimental setup for three-dimensional processing of the materials, as shown schematically in Fig. 2, consisting of: fiber ytterbium femtosecond laser (*1*) (Antaus-20W-20u/1M, Avesta Ltd.) with the wavelength $\lambda = 1030$ nm, pulse duration $\tau = 220$ fs and the maximum pulse frequency $\nu = 1$ MHz, periscope (*2*) (Avesta PVH-DP); mirrors (*3*) with dielectric coating ($R > 99\%$), focusing optics (*4*), three coordinate system (*5*) (Thorlabs), that ensures the sample scanning speed (*6*) in the XYZ field from 0.1 to 50.0 mm/s with

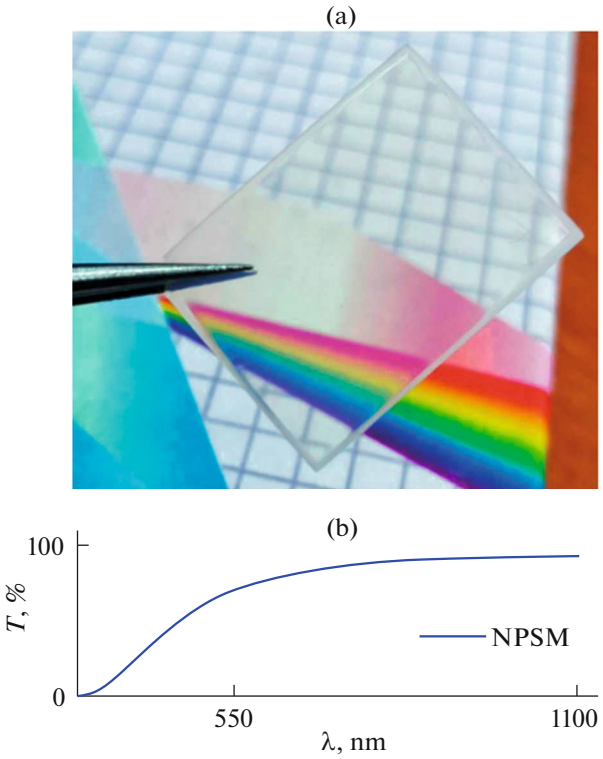

Fig. 1. (a) Photo of NPSM; (b) transmission spectrum within the range of 300–1100 nm.

the minimum shift of 0.5 μm, and PC (*7*). Selection of optics (*4*) for focusing laser radiation depended on the set task. Radiation was focused by means of objective for writing waveguides and microchannels (LOMO, 60x, NA = 0.85). Flat-convex lens (Thorlabs LA4102, $f' = 200$ mm) was used for writing of barriers.

Experemental scheme: laser radiation (*1*) passed through the system of mirrors (*2*, *3*) is focused by lens or objective (4) into the volume of the NPSM plate (*5*). NPSM plate is secured onto three-coordinate system (*6*) for the sample positioning relative to focused laser beam. Simultaneously with the laser switching ON (*1*) the coordinate system starts (*6*) moving the sample according to the trajectory set by PC in the software for control of laser source and the coordinate system "Laserbench v2.0" [19]. The writing was performed at the depth of 400 μm from the NPSM plate surface at the constant ν = 200 kHz.

If channel waveguides and barriers were written in 1 stage of the straight-line scanning by the coordinate X all over the NPSM plate length, then, fabrication of microchannel was performed for several stages, as shown schematically in Fig. 3a: (i) direct laser writing of tracks in the NPSM decompaction mode [20] and (ii) subsequent cleaning of the written tracks from the destruction products in distilled water under the effect of ultrasound (ultrasonic bath, Sapphire) at the temperature of 31°C. Additionally, thermal treatment

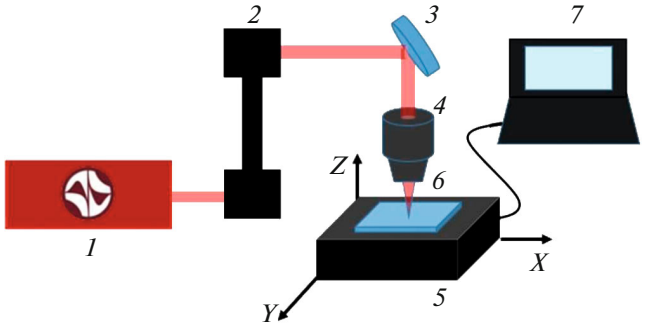

Fig. 2. Diagram of experimental setup for direct laser writing: femtosecond laser (*1*), periscope (*2*), dielectric mirrors (*3*), objective (*4*), three-coordinate system (*5*), sample (*6*), PC (*7*).

(700°C, 1 h) of microchannels was performed for demonstration of the possibility of evening the inner relief of the microchannels.

Evaluation of the barriers permeability was performed with merging the NPSM sample with barriers into water solution of thionine organic dye with the mass fraction of 0.009% (Fig. 3b). The procedure refers to securing of the NPSM plate with the written barriers above the container with organic dye. When a part of the plate is submerged into pigment without touching the recorded barriers, a nanoporous frame is filled with solution. The barrier divides the NPSM plate physically into sectors, in our case, with the area of ~5 mm^2, and prevents propagation of the pigment molecules. Subsequent examination of the NPSM plate under microscope allows to trace non-permeability of the barrier relative to the dye molecules. Such method of study allows to detect pigment molecules propagated beyond the barrier, without analyzing the substance spectrum.

Test of waveguides was performed on the setup, whose diagram is shown in Fig. 3c, and which we used earlier for the study of waveguides in porous glass [17].

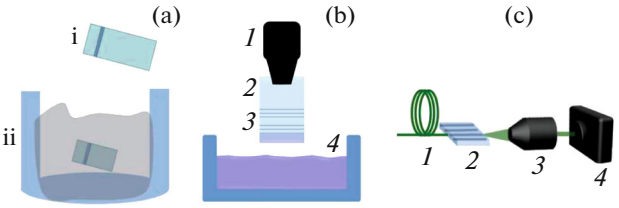

Fig. 3. Schematic flow diagram of the test of created optic-fluid elements: (a) two stages of microchannels formation: (i)—writing of tracks in the NPSM material decompaction mode, and (ii)—cleaning of the decompaction tracks in water from the debris; (b) study of permeability of barriers: *1*—holder, *2*—NPSM, *3*—barriers in NPSM, *4*—pigment solution; (c) introduction of radiation into waveguides: *1*—optic fiber, *2*—NPSM with channel waveguides, *3*—objective (40x, NA0.65), *5*—CMOS camera Gentec 3M.

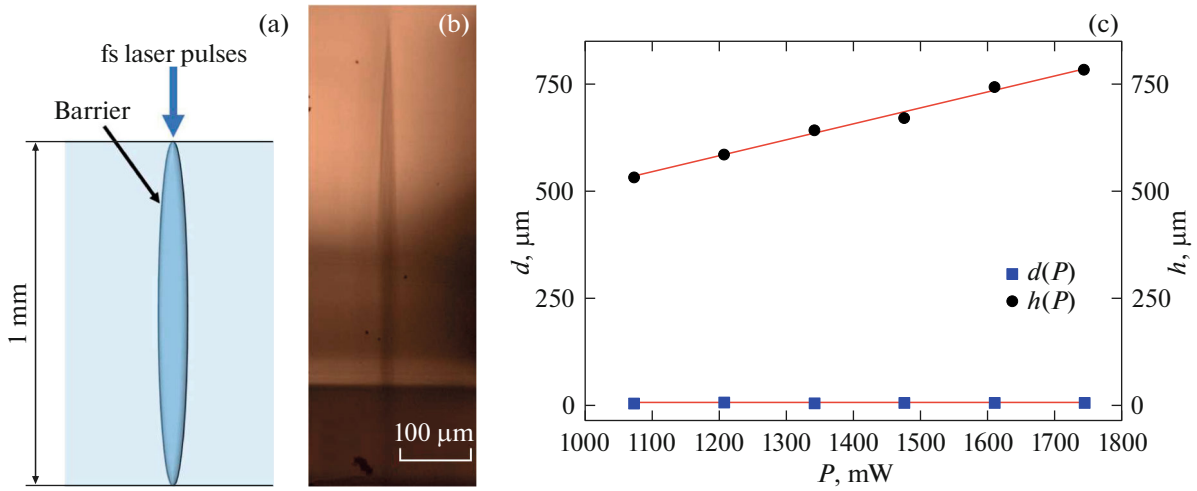

Fig. 4. (a) Schematic diagram of the barrier in a NPSM plate; (b) microphotograph of the barrier recorded at the power of 1540 mW and scanning speed of 1 mm/s; (c) dependence of the barrier height (h) and (d) width in cross-section on the radiation power.

Diagram composition: optical fiber (Thorlabs, FS-SN-3224) with the diameter of mod field 4 μm (*1*), NPSM plate with the waveguides recorded within the volume (*2*), objective (40X, 0.65 NA) (*3*) and CMOS camera (Gentec 3M) (*4*). Radiation introduction ($\lambda = 532$ nm) into the channel waveguide was performed by means of fiber (*1*), whose low cross-section and the possibility to approach closely to the sample enable introduction of radiation with the minimum losses. The near-field distribution of intensity is registered by means of CMOS camera (*3*) with the objective (*4*).

Microphotographs of recorded elements were made using the microscope Axio Imager A1m (Carl Zeiss). The NPSM transmission spectrum was obtained by spectrophotometer SF-56 (LOMO). NPSM plate faces processing after laser writing was performed on the grinding and polishing machine (Buehler MetaServ 250).

RESULTS AND DISCUSSION

Barriers Writing

The tracks with compacted structure and elongated form in the section were formed under the effect of femtosecond laser pulses at the constant frequency of 200 kHz and with different value of radiation power (1000–1750 mW) and scanning speeds (0.5–20 mm/s). It was expected to make a region with compaction all over the thickness of the NPSM plate (Fig. 4a). The calculated Rayleigh length was 5.8 mm. However, focusing and defocusing of radiation during modification of the processed material significantly decreases the size of the formed modification region in dielectric [21] (Fig. 4b). As a result of laser writing we made barriers with the maximum height of ~750 μm. All the created barriers look identically: elongated region of modification extended in the central part and narrowed in the superior and inferior parts. Dependence of the length and width of the barriers in cross section was made for various values of power (Fig. 4c). With the increase of the power of laser, the height of barriers rises from 500 to 800 μm, wherein their width remains within the limits from 8 to 10 μm.

The barrier permeability was evaluated as a result of NPSM impregnation with the solution of thionine dye (Figs. 5a, 5c). When placing NPSM in the solution the matrix starts picking the pigment molecules as a result of diffusion processes, and upon expiration of a time, the molecules fill porous space with pigment. As a result of the barrier formation in NPSM we succeeded in stopping the pigment molecules propagation (Fig. 5b).

At this stage the recorded barriers are not absolutely impermeable, because it was found that during sample impregnation with the pigment solution, water propagated beyond the barrier, because its molecules have a lower size than the size of pores in the region of the barrier.

Writing of Channel Waveguides

As a result of femtosecond laser writing (ν = 200 kHz, P = 17–170 mW, v = 15 mm/s), channel optical waveguides were fabricated inside the NPSM plate volume. Figure 6a shows appearance of the cross-section of standard waveguides formed as a result of the increase of the refraction index in the modified region of the material. When studying under microscope of transversal and longitudinal sections of the fabricated elements, the dependence of the width

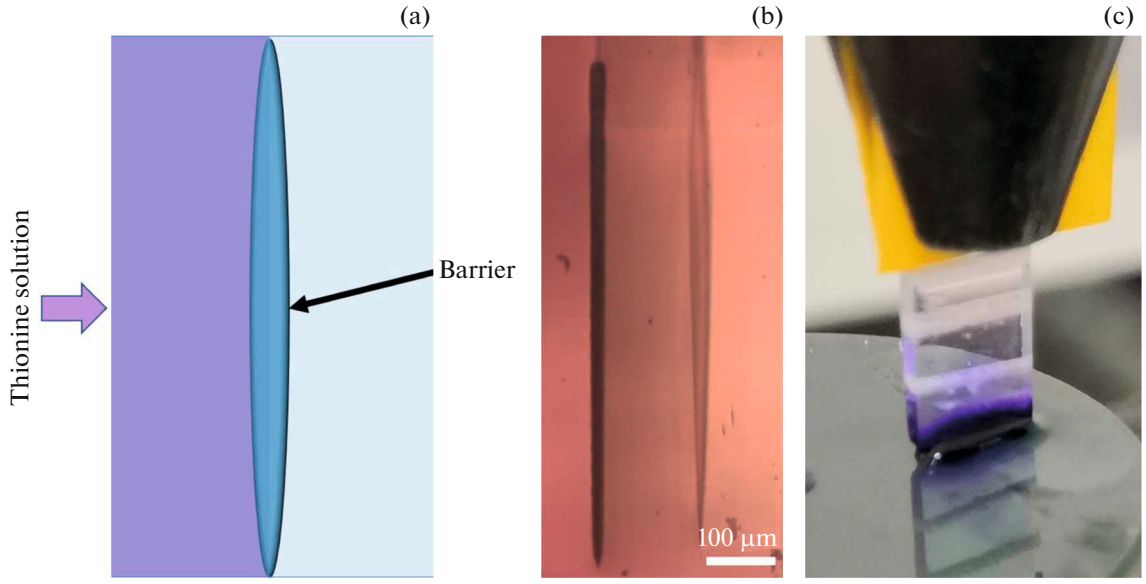

Fig. 5. (a) schematic diagram of the barrier functioning for retention of the pigment molecules; (b) microphotograph of the cross-section of NPSM plate after impregnation with thionine solution (pigment molecules propagate from the left to the right); (c) photograph of the impregnation process of the NPSM plate with barrier.

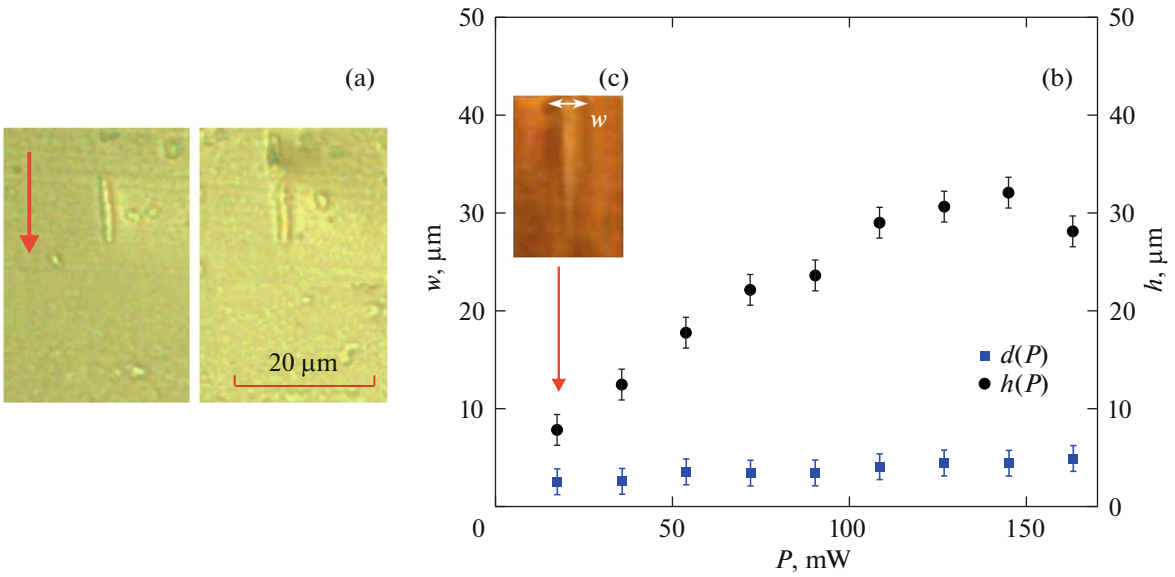

Fig. 6. (a) Microphotographs of asymmetric waveguides (end view, the arrow indicates direction of laser beam in the process of laser direct writing); (b) dependence of the width of cross-section of waveguide on the power of laser radiation; (c) cross-section of waveguide with the power of laser radiation 17–50 mW.

(*w*) and height (*h*) of their section on the laser radiation power (*P*) was found (Fig. 6b). It was noted that as far as the radiation power is increasing, asymmetric waveguides were formed with the aspect ratio of 9.0.

Next, by using the experimental flow diagram shown in Fig. 3c, we studied propagation of laser radiation with the wavelengths 532 nm, 20 mW in waveguides. The photograph of the process of coupling radiation with channel waveguide in the NPSM plate is shown in Fig. 7a. As a result, near-field distribution of intensity at the exit from waveguide was registered (Fig. 7b). It was noted that at the distance of 5–10 μm between waveguides, radiation is pumped to neighboring waveguide (Fig. 7b). On the one hand, it is related with low contrast of the refraction index of waveguide, which is manifested in optical losses. On the other

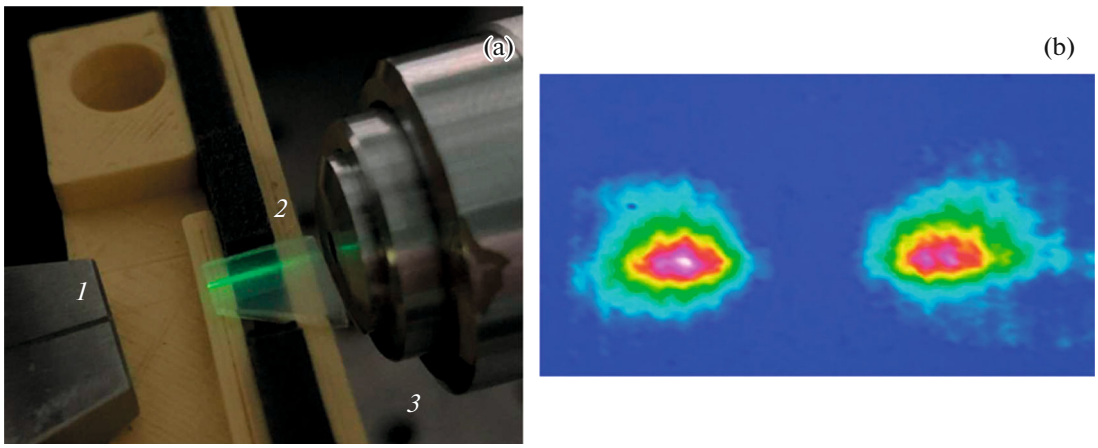

Fig. 7. (a) Photograph of the process of the radiation introduction into waveguide: *1*—fiber, *2*—NPSM with a set of channel waveguides with the placement period of 10 μm and *3*—objective; (b) near-field distribution of intensity at the exit from the waveguide.

hand, the effect of pumping of coherent radiation between optical waveguides is demanded for the study of quantum transition in so called photon arrays [22]. Nanoporous silicate frame between such

channel waveguides could be promising from the point of view of filling it with substances having nonlinear optical response or luminescent properties. This requires further study.

Microchannels Writing

Fabrication of a microchannel inside NPSM plate occurs in 2 stages. At the first stage, laser writing of tracks is performed in the NPSM decompaction mode. Particles of destructed material are formed within the cross-section of the formed track. At the second stage, decompaction tracks are cleaned from debris. Main goal is to preserve the nanoporous structure around the microchannel and to clean the structures without chemical etching. In solid glasses the stage of cleaning of such tracks is performed in strong acids or alkali, which modifies geometry of the microchannel [23] and/or there are limitations of its length [8]. The decompaction tracks were recorded at the constant pulse repetition frequency of 200 kHz, scanning speed of 20 mm/s, but at various radiation power from 170 to 640 mW. One of the criteria of the mode selection for laser writing is formation of continuous and uniform (±0.5 μm) decompaction track all over the writing trajectory. A fragment of such tracks is shown in Fig. 8a. Homogeneous illumination of the fabricated structure when studying in crossed polarizer and analyzer indicates the presence of defects on the track periphery (Fig. 8b). It is assumed that this illuminated region will be cleaned in water under the effect of ultrasound. Before cleaning the sample in water, NPSM plate faces were polished to open these tracks (Fig. 8c) and to ensure distilled water ingress during the channel cleaning process. Also, the study of the track geometry modification due to the laser radiation power was performed. The obtained results indicate that the track geometry (height (h) and width (d)) can be varied within a wide range—from 4 to 20 μm and from 4 μm to 14 pm, accordingly (Fig. 8d).

Then, the NPSM plate with decompaction tracks was placed into ultrasonic bath filled with distilled water. Microchannels were observed by means of a microscope every 15 min of the ultrasound action. Upon expiration of 15 min, the microchannel was cleared significantly all over its length (Fig. 9a). Then, ultrasound was in action for additional 120 min. One can note, there were no considerable changes in the channel cross section after 60 min (Fig. 9b). As we can see in the microphoto, clearance regions appeared in track, which, probably, are filled with water, since after the sample drying (100°C) a notable dissipation appeared from the microchannels when viewing through optical microscope (Fig. 9c). According to microphotographs, there are uncleared regions on the periphery, most likely, in the form of micropores, according to our preliminary studies in [24]. More detailed review is possible by means of electronic microscopy. Nevertheless, in order to exclude consolidation of the destruction products, one should apply lower frequency of the pulse repetition [25].

Then, we performed heat treatment of NPSM with microchannels in furnace at the temperature higher than the temperature of vitrifying (700°C during 1 h). Microphotographs indicate significant shrinkage (by 0.65 times) of microchannels (Fig. 9d). However, one can note that tracks fabricated at the power of 200–250 mW had more free space, which lead to expansion of the microchannel as a result of heat treatment up to 16 μm, meanwhile the channels with lower free space were virtually collapsing and left only central part. Moreover, heat treatment lead to considerable evening of the inner surface of channel. The channel treatment temperature mode should be studied with more details

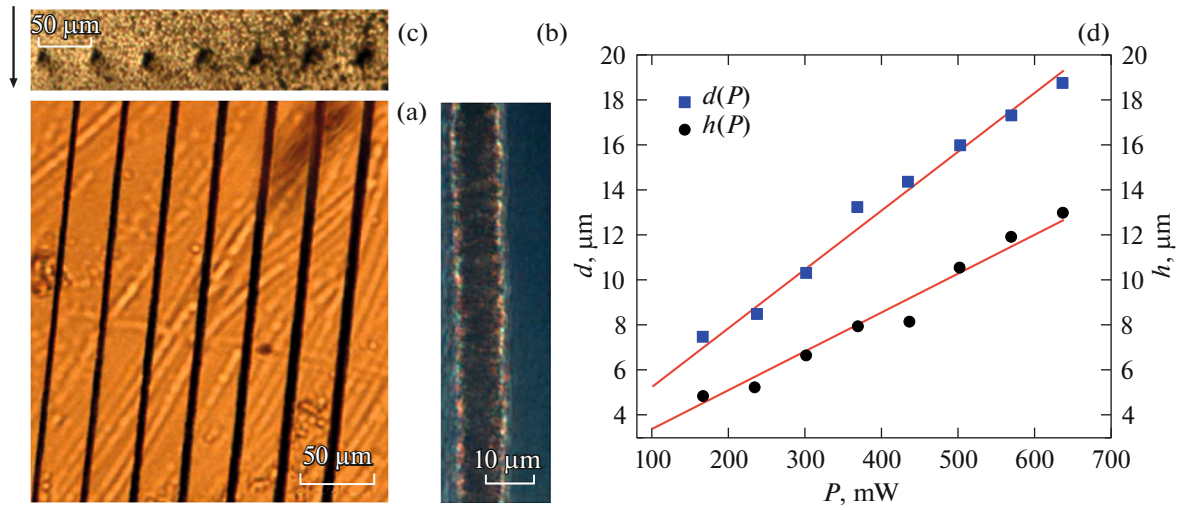

Fig. 8. (a) Microphotograph of the material decompaction tracks after laser writing (c) view of the cross-section after polishing, the arrow indicates direction of laser beam in the process of writing and (b) microphotograph of the decompaction track under crossed polarizer and analyzer; (d) the graph of dependence of the diameter and height of cross-section of microchannel on the laser power.

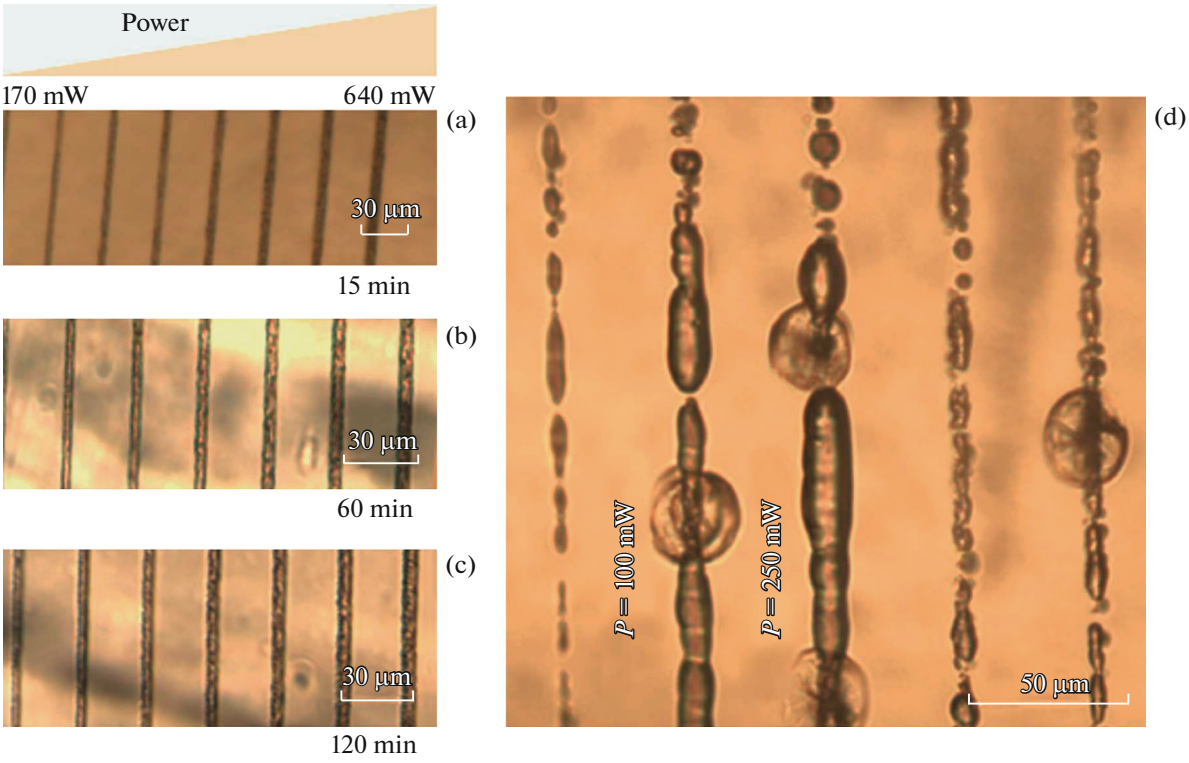

Fig. 9. Microphotograph of microchannels after cleaning in distilled water under the effect of ultrasound 15 (a), 60 (b) and 120 min (c), (d) after the sample heat treatment.

in order to determine the temperature, at which the microchannels is evened without collapsing. Smooth channels provide a laminar flow, which is demanded by the tasks of microfluidics [26].

Based on the published data [27], we may assume that longer microchannels will be harder to clean, since the destruction area could block the water flow. There are several ways of resolution of these prob-

lems—microchannel expansion, writing of additional channels with outlet at the glass surface or multi-pass writing.

CONCLUSION

The work demonstrated direct laser writing with the wavelength of 1030 nm, constant pulse duration of 220 fs and the pulse repetition rate of 200 kHz for three types of optofluidic elements inside the NPSM plate. The studied elements are the barriers, channel optic waveguides, and microchannels. Outer differences of the recorded elements is observed in microphotographs, as well as in the graphs of dependence of their sizes in cross-section on the power of laser radiation, where the curves are linear.

In particular, as far as the power of laser radiation is increased, the barrier height rises from 500 to 800 pm, however, its width remains constant (8–10 μm). The barriers testing confirmed retention of the thionine dye molecules in the region limited by the barrier. It is shown that the barrier is capable for stopping propagation of the dye molecules inside the NPSM plate. However, we noted selective permeability of the barrier depending on the size of molecules. For example, molecules of water have passed through the barrier.

Narrow focusing of laser radiation resulted in the writing of the first type channel waveguides. By controlling the power of laser radiation, we succeeded in change of the aspect ratio of the waveguide cross-section from 5.0 to 9.0. Introduction of radiation (532 nm, 20 mW) was done by using one-mode fiber. Near-field distribution was registered with the objective and CMOS camera. It was noted that when positioning waveguides at a distance from each other 5–10 μm the radiation is pumped from one channel to other.

The procedure is described and demonstrated as fabrication of microchannels in the NPSM plate, consisting of two stages. The first stage includes laser writing of tracks of nanoporous matrix decompaction, consisting of the material destruction products. The second stage includes cleaning of tracks in distilled water under the effect of ultrasound. It is shown that 15 min are enough for removal of the destruction products all over the channel length. However, there are destruction products remaining on the channel periphery. Additional stage of heat treatment confirmed that decompaction tracks recorded at the laser radiation power of 200–250 mW, contained less amount of the destruction products after the cleaning stage. Then, it is expedient to exclude consolidation of the destruction products by decrease of the pulse repetition frequency.

The obtained results are promising in the field of integration of optic, liquid and separating elements on a common silicate optically transparent matrix. Each presented element has additional benefit because of the surrounding nanoporous medium, which can be impregnated with organic molecules [28], photosensitive [29] and rare-earth [30] components, quantum dots [31] etc. in order to provide each element with unique optical properties.

FUNDING

Direct laser writing and study of integrated elements was performed from funds of the grant from Russian Research Foundation (project no. 20-71-10103). V.A. Yakimuk expresses his appreciation for supporting the studies of channel waveguides within the framework of financial support of the grant from NIRMA FT MF of the ITMO University.

CONFLICT OF INTEREST

The authors of this work declare that they have no conflict of interest.

REFERENCES

1. D. Tan, B. Zhang, J. Qiu, Laser & Photonics Reviews, **15** (9), 2000455 (2021). https://doi.org/10.1002/lpor.202000455
2. B. Zhang, L. Li, B. Wu, H. Liu, P. Wu, L. Wang, F. Chen, J. Lightwave Technology, **39** (5), 1438–1443 (2021). https://doi.org/10.1109/JLT.2020.3038438
3. G. L. Roth, S. Kefer, S. Hessler, C. Esen, R. Hellmann, J. Laser Micro/Nanoengineering, 16 (1), (2021). https://doi.org/10.2961/jlmn.2021.01.2009
4. Y. Cheng, Micromachines, **8** (2), 59 (2017). https://doi.org/10.3390/mi8020059
5. F. Sima, K. Sugioka, Nanophotonics (2021). https://doi.org/10.1515/nanoph-2021-0159
6. M. Macias-Montero, F. Munoz, B. Sotillo, J. del Hoyo, R. Ariza, P. Fernandez, J. Siegel, J. Solis, Sci. Rep., **11** (1), 1–12 (2021). https://doi.org/10.1038/s41598-021-87765-z
7. S. I. Kudryashov, P. A. Danilov, A. E. Rupasov, M. P. Smayev, A. N. Kirichenko, N. A. Smirnov, A. A. Ionin, A. S. Zolot'ko, R. A. Zakoldaev, Appl. Surface Sci., **568**, 150877 (2021). https://doi.org/10.1016/j .apsusc.2021.150877
8. Z. Liu, J. Xu, Z. Lin, J. Qi, X. Li, A. Zhang, J. Lin, J. Chen, Z. Fang, Y. Song, W. Chu, Y. Cheng, Optics & Laser Technology, **141**, 107118 (2021). https://doi.org/10.1016/j .optlastec.2021.107118
9. A. Schaap, T. Rohrlack, Y. Bellouard, Lab on a Chip, **12** (8), 1527–1532 (2012). https://doi.org/10.1039/c2lc21091f
10. J. Xu, K. Midorikawa, K. Sugioka, Laser Applications in Microelectronic and Optoelectronic Manufacturing, **XXI** (9735), 97350B (2016). https://doi.org/10.1117/12.2208842
11. V. Stankevic, G. Raciukaitis, J. Laser Micro/Nanoengineering, 9 (3), 1–5 (2014). https://doi.org/10.1364/OE.431306

12. J. Lapointe, M. Gagne, M.-J. Li, R. Kashyap, Optics Express, **22** (13), 15473–15483 (2014). https://doi.org/10.1364/OE.22.015473
13. L. Syedmoradi, M. Daneshpour, M. Alvandipour, F. A. Gomez, H. Hajghassem, K. Omidfar, Biosensors and Bioelectronics, **87**, 373–387 (2017). https://doi.org/10.1016/j.bios.2016.08.084
14. L. Capuano, R. M. Tiggelaar, J. W. Berenschot, J. G. E. Gardeniers, G. R. B. E. Romer, Optics and Lasers in Engineering, **133**, 106114 (2020). https://doi.org/10.1016/j.optlaseng.2020.106114
15. X. L. Guo, Y. Chen, H. L. Jiang, X. B. Qiu, D. L. Yu, Sensors, 18 (9), 3141 (2018). https://doi.org/10.3390/s18093141
16. T. T. Fernandez, S. Gross, K. Privat, B. Johnston, M. Withford, Advanced Functional Materials, **2103103** (2021). https://doi.org/10.1002/adfm.202103103
17. Z. Lijing, R. A. Zakoldaev, M. M. Sergeev, A. B. Petrov, V. P. Veiko, A. P. Alodjants, Nanomaterials, **11** (1), 123 (2021). https://doi.org/10.3390/nano11010123
18. O. V. Andreeva, I. E. Obyknovennaya, E. R. Gavrilyuk, A. A. Paramonov, A. P. Kushnarenko, J. Optical Technology, **72** (12), 916–922 (2005). https://doi.org/10.1364/JOT.72.000916
19. V. S. Rymkevich, R. A. Zakoldaev, M. M. Sergeev, V. V. Koval, Software for control of laser units and coordinate table "Laserbench v2.0". Certificate no. 2017612835 (2017).
20. H. Ma, R. A. Zakoldaev, A. Rudenko, M. M. Sergeev, V. P. Veiko, T. E. Itina, Optics Express, **25** (26), 33261–33270 (2017). https://doi.org/10.1364/OE.25.033261
21. K. Liao, W. Wang, X. Mei, B. Liu, Optics & Laser Technology, **142**, 107201 (2021). https://doi.org/10.1016/j.optlastec.2021.107201
22. N. N. Skryabin, S. A. Zhuravitskii, I. V. Dyakonov, M. Y. Saygin, S. S. Straupe, S. P. Kulik, In: *AIP Conference Proceedings* (AIP Publishing LLC, 2020), v. 2241, N 1, p. 020033. https://doi.org/10.1063/5.0011377
23. Z. Wang, H. Zheng, W. Zhou, Laser and Particle Beams, **27** (3), 521–528 (2009). https://doi.org/10.1017/S0263034609990255
24. T. E. Itina, R. A. Zakoldaev, M. M. Sergeev, H. Ma, S. I. Kudryashov, O. S. Medvedev, VP. Veiko, Optical Materials Express, **9** (11), 4379–4389 (2019). https://doi.org/10.1364/OME.9.004379
25. S. Nikumb, Q. Chen, C. Li, H. Reshef, H. Y. Zheng, H. Qiu, D. Low, Thin Solid Films, **477** (1–2), 216–221 (2005). https://doi.org/10.1016/j .tsf.2004.08.136
26. B. G. Belenkii, N. I. Komyak, V. E. Kurochkin, A. A. Evstrapov, V. L. Sukhanov, Sci. Instrument., **10** (3), 3–16 (2000).
27. Y. Liao, Y. Ju, L. Zhang, F. He, Q. Zhang, Y. Shen, D. Chen, Y. Cheng, Z. Xu, K. Sugioka, K. Midorikawa, Opt. Lett., **35** (19), 3225–3227 (2010). https://doi.org/10.1364/OL.35.003225
28. K. Ito, N. Kawamura, Y. Suzuki, Y. Y. Maruo, Microchemical J., **159**, 105428 (2020). https://doi.org/10.1016/j .microc.2020.105428
29. M. A. Girsova, L. N. Kurilenko, I. N. Anfimova, M. Y. Arsent'ev, F. Dikaya, E. A. Semenova, Russian Chemical Bulletin, **69** (5), 920–925 (2020). https://doi.org/10.1016/j.microc.2020.105428
30. L. D. Iskhakova, V. M. Mashinsky, F. O. Milovich, V. V. Velmiskin, E. A. Plastinin, S. V. Firstov, M. V. Lukashova, P. A. Somov, E. M. Dianov, J. Non-Crystalline Solids, **503**, 28–35 (2019). https://doi.org/10.1016/j.jnoncrysol.2018.09.022
31. A. P. Litvin, A. A. Babaev, P. S. Parfenov, E. V. Ushakova, M. A. Baranov, O. V. Andreeva, K. Berwick, A. V. Fedorov, A. V. Baranov, J. Phys. Chem. C, **121** (15), 8645–8652 (2017). https://doi.org/10.1021/acs.jpcc.7b01952